Nanosecond Switchable Polymerized Crystalline Colloidal Array Bragg Diffracting Materials

Guisheng Pan, R. Kesavamoorthy,† and Sanford A. Asher*

Contribution from the Department of Chemistry, University of Pittsburgh, Pittsburgh, Pennsylvania 15260

Received February 12, 1998

Abstract: We fabricated a mesoscopically periodic array of novel colloidal particles containing absorbing dye embedded in a polyacrylamide hydrogel through the use of crystalline colloidal self-assembly. These colloidal particles are highly fluorinated (see accompanying paper) and have a very low refractive index, which can be easily refractive index matched to a predominantly aqueous medium. Thus, we were able to prepare a material where the real part of the refractive index was matched, while preserving a periodic modulation of the imaginary part of the refractive index. Previously we theoretically predicted that such a material could be used as a nanosecond optical switch (Kasavamoorthy, Super, and Asher, *J. Appl. Phys.* **1992**, *71*, 1116), and more recently experimentally demonstrated this optical switching (Pan et al., *Phys. Rev. Lett.* **1997**, *78*, 3860). Under low light intensities the crystalline colloidal arrays (CCA) is refractive index matched to the medium and does not diffract. However, high incident intensity illumination within the dye absorption band heats the particles within nanoseconds to decrease their refractive index. This results in a mesoscopically periodic refractive index modulation with the periodicity of the CCA lattice. The array "pops up" to diffract light within 2.5 ns. These intelligent CCA hydrogels may have applications in optical limiting, optical computing, and nanosecond fast optical switching devices, etc.

Introduction

Dispersions of highly charged, monodisperse, submicrometer-sized colloidal particles can self-assemble into body-centered cubic (bcc) or face-centered cubic (fcc) crystalline colloidal arrays (CCAs) as a result of interparticle screened Coulombic repulsion.[1−6] The optical dielectric constant of these particles, in general, differs from that of the surrounding medium, which results in a periodic variation in the material's refractive index. This modulation in the refractive index results in Bragg diffraction, similar to the diffraction of X-rays from atomic and molecular crystals. A major difference occurs, however, in that the periodicity in the refractive index for the CCA is much larger than that found for atomic and molecular crystals; it occurs in the 10 nm to 3 μm length scale. Thus, the CCA efficiently diffracts electromagnetic radiation in the UV, visible, and near-IR spectral regions.[4,6] This unique property can be used to make devices such as narrow band optical rejection filters [4,7−11] and chemical sensing devices.[12]

We demonstrated recently that the CCA periodicity can also be used to fabricate nanosecond nonlinear optical switching and limiting devices.[13−16] The idea is to match the real part of the refractive index of dyed CCA particles to that of the medium. Thus, at low light intensities, no optical dielectric constant modulation occurs and light freely transmits. However, since the dyed particles have a thermal nonlinear dependence of their refractive index on the incident light intensity, at high light intensities the particle refractive index will diverge from that of the medium, and the periodic modulation of the real part of the refractive index will "pop up" to diffract the high-intensity incident light. For a 5 ns pulsed laser beam of 10 MW/cm^2, our calculations[15] showed that the refractive index of the particles would diverge sufficiently from that of the medium that a perfectly ordered CCA would diffract >90% of the incident light within 5 ns.

In the preceding paper,[17] we described the synthesis of monodisperse, low refractive index, dyed, highly charged colloidal particles consisting of poly(1H,1H-heptafluorobutyl methacrylate). These particles, have a sufficiently low refractive index ($n_D = 1.3860$) that they can be easily matched to a predominantly aqueous medium. We also described the self-assembly of these particles into a CCA and the immobilization of this dyed CCA into a polyacrylamide hydrogel matrix (PCCA). We

* To whom correspondence should be sent. Phone: 412-624-8570. Fax: 412-624-0588. E-mail: Asher+@pitt.edu.

† Permanent address: Materials Science Division, Indira Gandhi Centre for atomic Research, Kalpakkam 603 102, Tamil Nadu, India.

(1) Krieger, I. M.; O'Neill, F. M. *J. Am. Chem. Soc.* **1968**, *90*, 3114−3120. (b) Hiltner, P. A.; Krieger, I. M. *J. Phys. Chem.* **1969**, *73*, 2386−2389.

(2) Clark, N. A.; Hurd, A. J.; Ackerson, B. J. *Nature* **1979**, *281*, 57−60.

(3) Pieranski, P. *Contemp. Phys.* **1983**, *24*, 25−73.

(4) Flaugh, P. L.; O'Donnell, S. E.; Asher, S. A. *Appl. Spectrosc.* **1984**, *38*, 847−850.

(5) Sood, A. K. In *Solid State Physics*; Ehrenreich, H., Turnbull, D., Eds.; Academic Press: New York, 1991; Vol. 45, pp 1−73.

(6) Carlson R. J.; Asher, S. A. *Appl. Spectrosc.* **1984**, *38*, 297−304.

(7) Asher, S. A.; Flaugh, P. L.; Washinger, G. *Spectroscopy* **1986**, *1*, 26−31.

(8) Asher, S. A. U.S. Patents 1986, Nos. 4 627 689 and 4 632 517.

(9) Spry, R. J.; Kosan, D. J. *Appl. Spec*trosc. **1986**, *40*, 782−784.

(10) Sankara, H. B.; Jethmalani, J. M.; Ford, W. T. *Chem. Mater.* **1994**, *6*, 362.

(11) Weissman, J. M.; Sunkara, H. B.; Tse, A. S.; Asher, S. A. *Science* **1996**, *274*, 959−960.

(12) Holtz, J. H.; Asher, S. A. *Nature* **1997**, *389*, 829−832.

(13) Runquist, P. A.; Jagannathan, S.; Kesavamoorthy, R.; Brnardic, C.; Xu, S.; Asher, S. A. *J. Chem. Phys.* **1991**, *94*, 711−717.

(14) Kesavamoorthy, R.; Jagannathan, S.; Rundquist, P. A.; Asher, S. A. *J. Chem. Phys.* **1991**, *94*, 5172−5179.

(15) Kesavamoorthy, R.; Super, M. S.; Asher, S. A. *J. Appl. Phys.* **1992**, *71*, 1116−1123.

(16) Pan, G.; Kesavamoorthy, R.; Asher, S. *Phy. Rev. Lett.* **1997**, *78*, 3860−3863.

(17) See preceding article in this journal.

S0002-7863(98)00481-8 CCC: $15.00
Published on Web 06/20/1998

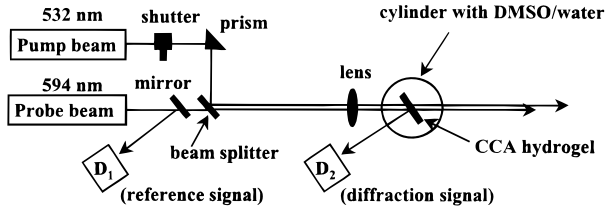

Figure 1. Experimental setup of nonlinear optical diffraction switching. A PCCA sample was mounted on an aluminum frame, which was placed in a glass cylinder containing a mixture of water and DMSO. The 532 nm pump and 594 nm probe beams (~3.5 ns duration) were collinear and focused onto the PCCA sample. The Bragg diffracted probe intensities were measured by photodiode D_2 and normalized to the incident probe intensity measured by photodiode D_1. R_{off} and R_{on}, the normalized diffracted probe beam, were measured in the absence and presence of the pump beam, respectively. The diffraction switching ratio, R_{on}/R_{off}, was monitored as a function of pump energy.

can easily adjust the refractive index of the medium by replacing part of the aqueous medium within the hydrogel. This system allows us to easily fine-tune the refractive index mismatch between the particles and the medium.

In this paper, we describe the optical nonlinear response of this PCCA and characterize the nanosecond optical limiting and switching.

Experimental Section

Monodisperse poly(1H,1H-heptafluorobutyl methacrylate) (PFBMA) particles were prepared as described in the preceding paper.[17] The particle diameter was measured to be 138 nm by TEM. The particle surface charge was 1850 charges per particle. These particles were dialyzed and ion exchanged to form a CCA. A PCCA (sample A) was prepared by photopolymerization of a CCA of 1.5827 g of the above colloid, 1.9323 g of ultrapure water, 0.3451 g acrylamide (monomer), 0.0234 g of N,N′-methylenebisacrylamide (cross-linker), and 0.0022 g of diethoxyacetophenone (UV photoinitiator) between two parallel quartz plates separated by a 800 μm thick Parafilm spacer. Sample A contained 9.62% volume fraction of particles. We also prepared a dyed PCCA (sample B) consisting of a 37.23% volume fraction of 225 nm diameter particles by following the above procedure. In addition, we prepared an 800 μm thick PCCA containing 10.05% volume fraction of undyed PFBMA spheres by utilizing 170 nm diameter particles. The optical extinction spectra (OES), with the incident light normal to the disk surface, were recorded by using a Perkin-Elmer Lambda 9 UV/VIS/NIR spectrophotometer.

A circular PCCA disk of 1.6 cm diameter was cut and mounted vertically on a metal frame. This disk was immersed in a water/DMSO solution contained in a cylindrical glass tank. Figure 1 shows the experimental setup which monitored the diffraction switching. The PCCA surface was tilted from the normal by ~20° in order to Bragg diffract a 594 nm probe beam from a dye laser, which was pumped by a 532 nm, 3.5 ns pulse width YAG laser (Coherent Inc. Infinity). The 532 nm YAG pump beam was used to switch on the PCCA diffraction. The pump and the probe beams were made collinear and focused onto a 100 μm radius spot on the PCCA sample. The probe beam was delayed with respect to the pump by 2.5 ns. The diffracted probe energy (I_2), as measured by photodiode D_2, was normalized to the incident probe energy (I_1), as measured by photodiode D_1, since the dye laser output fluctuates from one pulse to another by ~6%. R_{off} and R_{on}, the normalized diffracted probe beam intensities in the absence and presence of the pump beam, respectively, are defined as

$$R_{off} = (I_2/I_1)_{off} - (I_2/I_1)_{bck}$$

$$R_{on} = (I_2/I_1)_{on} - (I_2/I_1)_{leakage} - (I_2/I_1)_{bck} \quad (1)$$

where $(I_2/I_1)_{off}$ and $(I_2/I_1)_{on}$ are the normalized signals in the absence and presence of the pump beam, respectively. $(I_2/I_1)_{leakage}$ is the normalized leakage pump beam signal in the absence of the probe beam, $(I_2/I_1)_{bck}$ is the normalized background signal in the absence of both the probe and the pump beams. Each measurement (R_{on}/R_{off}) was averaged over 20 pulses, and the standard deviation was calculated. An absorbing filter placed in front of D_2 removed most of the 532 nm scattered pump beam. The remaining leakage of the scattered pump beam into D_2 was numerically removed from the measured R_{on} as shown in eq 1.

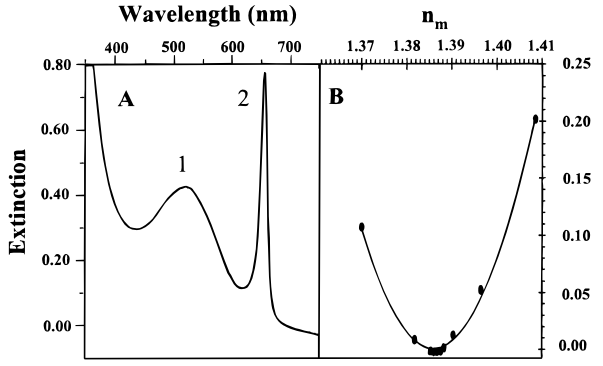

Figure 2. (A) Optical extinction spectrum of 138 nm diameter dyed poly(1H,1H-heptafluorobutyl methacrylate) PCCA in water. Peak 1 derives from absorption of the acylated Oil Blue N dye which is covalently bound to the particles. Peak 2 is the PCCA Bragg diffraction band. The spectrum was recorded in a UV−visible−near-IR spectrophotometer with the PCCA surface normal to the incident light beam. (B) Extinction of dyed PCCA (sample A) as a function of medium refractive index. The data (filled circles) are best fit to a parabolic curve: $A = 405.85(n_m - 1.3860)^2 + 0.0063$ where n_m is the medium refractive index and 1.3860 is the colloidal particle refractive index.

Results and Discussion

Figure 2A shows the OES of the PCCA in a DMSO/water solution at normal incidence, while Figure 2B shows the dependence of the maximum value of this extinction at 656 nm, as a function of the hydrogel medium refractive index (n_m). The 530 nm peak results from the dye absorption band. The diffraction of the incident beam almost follows Bragg law:

$$M\lambda_0 = 2nd_{hkl} \sin \theta_B \quad (2)$$

where M is the diffraction order and λ_0 is the Bragg diffracted wavelength in air. d_{hkl} is the interplanar spacing of the lattice plane with Miller indices (hkl). θ_B is the Bragg glancing angle of the incident beam relative to the (hkl) plane inside the crystal. n is the average refractive index of the PCCA which is given by

$$n = n_p\Phi_p + n_m(1 - \Phi_p) \quad (3)$$

where n_p is the particle refractive index (1.3860). Φ_p is the particle volume fraction in the PCCA. n_m is the hydrogel medium refractive index given by

$$n_m = 1.543x + n_{mix}(1 - x) \quad (4)$$

where 1.543 is the refractive index of polyacrylamide. x is the volume fraction occupied by the polyacrylamide hydrogel network in the medium, and n_{mix} is the measured refractive index of the DMSO/water solution. n_{mix} can be varied by varying the fraction, y, of DMSO in water:

$$n_{mix} = 1.479y + 1.333(1 - y) \quad (5)$$

where 1.479 and 1.333 are the refractive indexes of DMSO

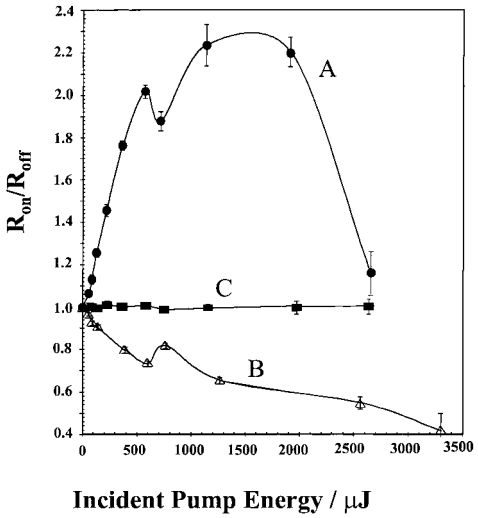

Figure 3. Pump beam energy dependence of R_{on}/R_{off} for the case of over- and under-index matching conditions. The probe beam was delayed by 2.5 ns compared to the pump beam. The pump beam spot size on the sample was a 100 μm radius. Curve A and B were measured for a dyed PCCA with n_m adjusted to 1.3902 and 1.3817, respectively; curve C was measured for an undyed PCCA at $n_m = 1.3874$.

and water, respectively. The extinction is defined by

$$E = -\log[1 - (I_D/I_0)] \tag{6}$$

where I_0 is the incident light intensity, I_D is the diffracted intensity. The extinction was best fit to a parabola:

$$E = a_1(n_m - n_p)^2 + b_1 \tag{7}$$

We found $x = 0.0301$, $a_1 = 405.85$, $b_1 = 0.0063$. The minimum value of E occurs when $n_m = n_p$.

We placed the PCCA in the sample chamber, adjusted the medium to the appropriate refractive index, and made the pump and probe beams coincident on the sample. Figure 3 shows the measured ratio of the diffraction of the probe beam in the presence and absence of the pump beam. Curve A was obtained for an over-index matched (n_m(1.3902) > n_p(1.3860)) PCCA, while curve B was obtained for an under-index matched (n_m-(1.3817) < n_p(1.3860)) PCCA, and curve C was obtained for an undyed PCCA with $n_m = 1.3817$. The signal, R_{on}/R_{off}, is independent of the pump energy for the undyed PCCA, since the undyed colloidal spheres do not absorb the pump. Thus, their temperature and n_p do not change; hence, no change occurs in the diffraction efficiency with increasing pump energy.

Curves A and B clearly indicate an optically nonlinear response of the dyed PCCA. As the pump beam heats the CCA, the diffraction efficiency increases when it is over-index matched ($n_m > n_p$), but decreases when it is under-index matched ($n_m < n_p$). The dyed CCA particles absorb the pump energy and heat up to decrease n_p, since $dn_p/dT < 0$. The over-index matched particles show an increasing refractive index mismatch as the pump pulse energy increases, and the particle refractive index decreases; this results in increased diffraction. In contrast, the under-index matched CCA becomes more matched on pump beam heating, which causes the diffraction to decrease.

A measurement of the transmitted pump energy indicates that the particles in the PCCA absorb 34% of the incident pump energy, which is identical to that calculated from the dye absorption at $\lambda = 532$ nm shown in Figure 2A. Assuming that this energy was absorbed uniformly by the CCA particles in the volume illuminated by the pump beam, the temperature increase (ΔT) can be calculated:

$$\Delta T = \frac{f_1 f_2 \Delta E}{mC} \tag{8}$$

where ΔE is the average pump pulse energy, f_1 is the fraction of the incident light energy that enters and is absorbed by the PCCA (34%), f_2 is the energy loss coefficient due to the reflection from the front surface of the container wall (96%), and C_p is the heat capacity of the polymer making up the particles. Since the PCCA was tilted from normal by ~20°, the illuminated total mass of particles by the pump beam is given by

$$m = N\left(\frac{\pi r^2 l_0}{\cos 20°}\right)\left(\frac{\pi {d_0}^3}{6}\right) \tag{9}$$

where r is the pump beam radius at normal incidence on the PCCA and l_0 is the PCCA thickness. d_0 is the particle diameter. There is insignificant refraction of light within the sample due to the close matching of the refractive index of the surrounding DMSO/water solution and the PCCA sample. N, the particle concentration (6.11×10^{13}/cm^3) was obtained from the calculated value of d_{hkl}, using eq 2, given the 648 nm measured diffraction wavelength, and that $n = 1.3926$. By inserting $\Delta E = 570$ μJ, $C_p = 1.15$ J K-1 g^{-1}, $r = 100$ μm, $l_0 = 800$ μm, and $d_0 = 138$ nm into eqs 8 and 9, the particle temperature increase at an incident pump pulse energy of 570 μJ, which corresponds to the first dip (peak) in curve A (B) of Figure 3, was calculated to be 46 °C. Hence, the calculated particle temperature was 69 °C. Both the dip in A, and the peak in B of the diffracted probe energy ratio, R_{on}/R_{off} occurs at 570 μJ. This calculated particle temperature of 69 °C is close to the 62 °C measured T_g value for these particles.[17]

n_p should continuously decrease with increasing particle temperature. Thus, we interpret the dip (peak) in the Figure 3A (B) curve in the over- (under-) refractive index matched sample at pump energies of ~570 μJ to indicate a region where the pump heating does not continuously increase with increasing pump energy. The fact that this pump energy corresponds to the T_g of the particles, suggests that this phase transition is associated with the phenomenon. We propose that residual crystalline order in the sphere polymer melts at T_g, causing a discontinuous particle volume increase, that induces turbulent flow around the particle, which transiently cools the particle and increases the temperature of the medium around it. Thus, the particle temperature would decrease slightly, and the medium temperature would increase slightly. This would increase n_p and lower n_m, giving rise to the observed dip (peak) in curve A (B) of Figure 3.

As the pump energy continues to increase the diffraction efficiency continues to increase (decrease) after the T_g dip (peak), due to further increases in particle temperature, and further decreases in particle refractive index, up to pump energies of ~1500 μJ. As long as the pump energy is maintained below ~1500 μJ, the PCCA response is fully reproducible and there is no evidence of degradation. However, for pump energies above 1500 μJ, the PCCA undergoes irreversible damage, which results in irreversible diffraction efficiency decreases for both curves A and B of Figure 3. This irreversible PCCA damage appears to result from damage to the array of particles, since we observe damage to a liquid dispersion of these particles if they are illuminated with 1000 pulses of 2000 μJ pump energy focused to a 100 μm spot radius.

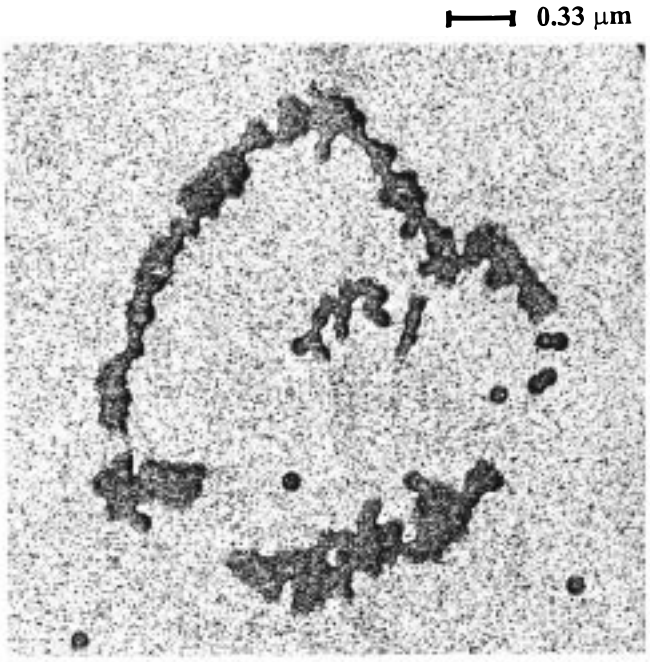

Figure 4. SEM picture of dyed poly(1H,2H-heptafluorobutyl methacrylate) colloidal spheres after irradiation by a 2 mJ, 532 nm pump beam. The particles were destroyed.

This degradation is evident in the Figure 4 SEM measurements of the colloid dispersion, which was dried on a glass plate and gold coated. No change in diffraction occurs in the absence of dye in the particles.

Although we calculated that essentially all of the incident light should be diffracted at pump energies of 10 MW/cm^2, we observe that the biggest R_{on}/R_{off} achieved is only 3.0 at T_g. Without the pump, the system is poised to diffract ~0.6% of the probe beam. Thus, only ~2% of the probe beam is diffracted in the presence of the pump.

Figure 5 shows the dependence of the ratio of light diffracted in the presence versus absence of the pump beam, as a function of the index mismatch between the medium and the particles ($n_m - n_p$), for a pump beam energy which heats the PCCA particles to T_g. The solid line in the figure represents the experimental data, while the dotted line was calculated using eqs 6 and 7, and the measured refractive indexes for the particles at T_g:

$$\frac{R_{on}}{R_{off}} = \frac{1 - 10^{-E_{on}}}{1 - 10^{-E_{off}}} \qquad (10)$$

where $E_{off} = 405.85(n_m - 1.3860)^2 + 0.0063$, while $E_{on} = 405.85(n_m - 1.3810)^2 + 0.0063$, where 1.3860 is the particle refractive index at room temperature ($T_0 = 23$ °C), and 1.3810 is the particle refractive index at T_g calculated from our measured dn_p/dT value (-1.39×10^{-4}/°C). As shown in Figure 5, the maximum diffraction ratio occurs for exact initial refractive index matching. The diffraction ratio decreases when the particle has an initial refractive index above the medium; heating causes a closer refractive index match. For $n_m > n_p$, R_{on}/R_{off} decreases as the mismatch increases, since the R_{off} value becomes larger as n_m increases. Our calculated R_{on}/R_{off} values mimic the pump−probe experimental data and the maximum diffraction occurs near the index matching point.

Figure 6 shows the pump delay time dependence of the diffraction efficiency at a pump beam energy which heats the particles to T_g. If the probe precedes the pump by 2.5 ns, no change in diffraction occurs compared to that in the absence of the pump beam. If the probe and pump coincide in time, the diffraction increases and continues to increase until the probe is delayed by 2.5 ns relative to the pump. Further delays cause the diffraction efficiency to decrease, and by a 10 ns delay little impact of pump heating is observed. The maximum diffraction is observed for a probe delay where there is a maximum temporal overlap between the heating and probe pulses. This ~5 ns observed time dependence is very similar to that which we theoretically predicted.[15]

Figure 7 shows the pump energy dependence for this same PCCA at $n_m = 1.3826$, when the pump was focused to a spot size of ~80 μm radius. Initially, the signal decreases because at zero pump energy $n_p > n_m$ ($\Delta n = -0.0034$), and pump

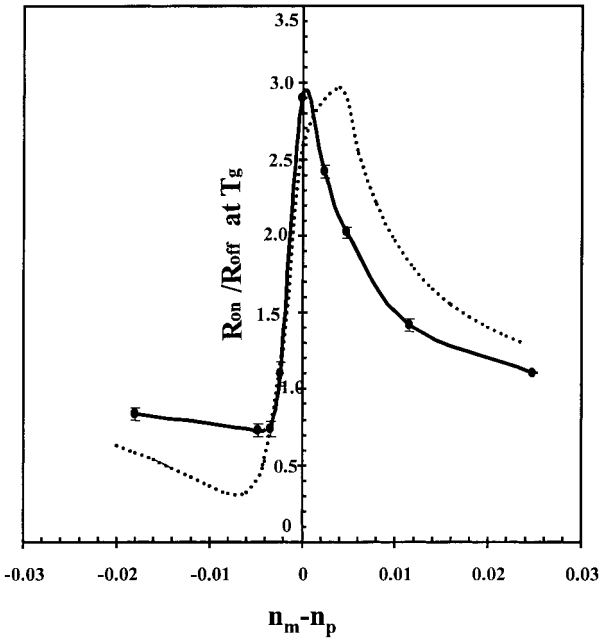

Figure 5. Dependence of R_{on}/R_{off} on the refractive index mismatch ($n_m - n_p$) when the PCCA is excited with sufficient pump energy to increase the particle temperature to T_g. The solid line through the experimental data points (filled circles) is a guide to the eye. The dotted line, which is calculated from eq 10, is qualitatively similar to that observed.

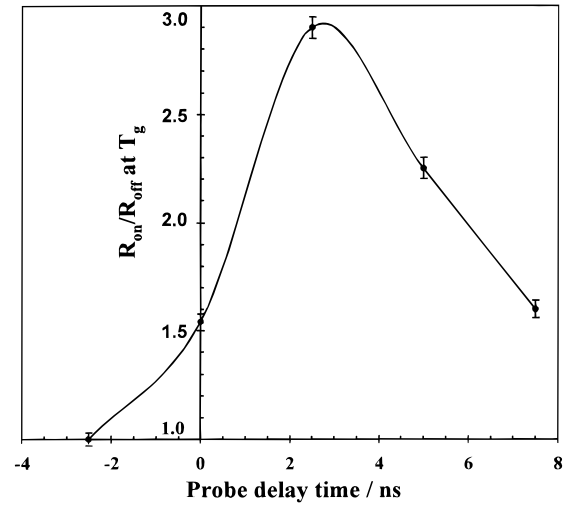

Figure 6. Dependence of R_{on}/R_{off} on the delay time between the probe and pump beams. The pump beam energy was set to heat the spheres to a temperature of T_g.

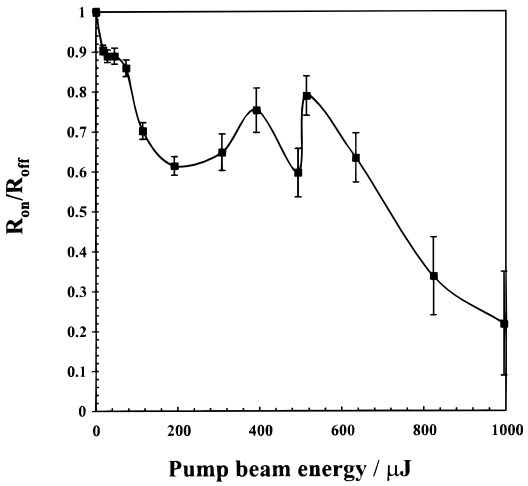

Figure 7. Pump beam energy dependence of R_{on}/R_{off} of dyed PCCA at $n_m = 1.3826$ for a 2.5 ns delayed probe when the pump was focused to an 80 μm radius spot.

heating increases the refractive index matching; the diffraction decreases until a pump energy of ~210 μJ, where the closest refractive index matching condition occurs. For this pump energy we calculate a temperature increase of 23 °C, which compares well with the 24 °C temperature rise, which would be required to match refractive indexes. The diffraction intensity increases for pump powers greater than ~210 μJ due to the decrease in n_p below n_m at these higher pump energies. The diffraction efficiency maximizes at 380 μJ, at the T_g point. The ratio of the pump energies required to heat the particle to T_g for 80 and 100 μm spot radius agrees well with the square of the focused spot area ratio. The T_g discontinuity, at ~500 μJ, and the decreasing diffraction at the highest pump energies are similar to that observed in Figure 3; at the highest powers the diffraction intensities decrease due to sample damage.

The CCA diffraction efficiency at any wavelength and incident angle depends on both the refractive index mismatch and the particle diameter. The maximum diffraction intensity should occur for largest diameter spheres, which indicates that we should operate at relatively high volume fractions. As shown in the Appendix we have found using Dynamical Diffraction Theory[18] that the maximum diffraction efficiency should occur for a particle volume fraction of 40.9% for PFBMA FCC crystals.

Thus, we attempted to increase the magnitude of the diffraction switching by utilizing a higher volume fraction PCCA. We prepared a high volume fraction (37.2%), 200 μm thick, dyed PCCA with large 225 nm diameter particles (sample B). Figure 8 shows the OES of this PCCA and the inset shows the index matching curve:

$$E = 496.53(n_m - 1.3860)^2 - 0.0011 \qquad (11)$$

Figure 9 shows the dependence of R_{on}/R_{off} for this PCCA on the pump beam energy (pump beam was focused to a ~50 μm radius spot). Curve A was obtained for an over-index matching condition ($n_m(1.3930) > n_p(1.3860)$, and curve B for an under-index matching condition ($n_m(1.3803) < n_p$). Again, we see the same trends as that in Figure 3. Figure 9 shows that T_g occurs at pump beam energy of ~230 μJ for curve A and ~150 μJ for curve B. The different pump energies required to achieve the particle T_g temperature results from small errors in the

(18) Zachariasen, W. H. *Theory of X-ray Diffraction in Crystals*; John Wiley and Sons: New York, 1946.

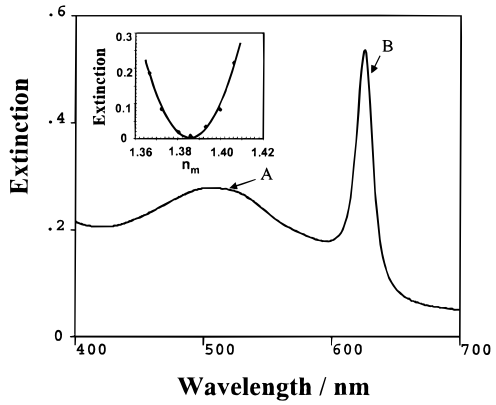

Figure 8. Optical extinction spectrum of a high volume fraction dyed PCCA in water. The 200 μm thick PCCA (sample B) had a particle volume fraction of 37.23% and a diameter of 225 nm. Peak A is the dye absorption band and peak B is the Bragg diffraction band. The insert shows the index matching curve of this PCCA in a DMSO/water mixture, and the fit to $E = 496.53(n_m - 1.3860)^2 - 0.0011$.

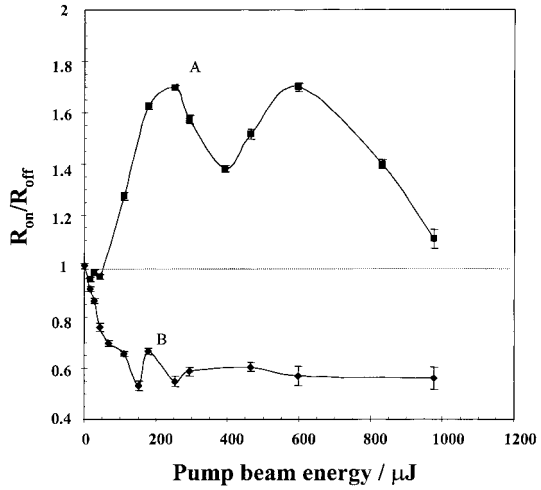

Figure 9. Pump beam energy dependence of R_{on}/R_{off} for over- and under-index matching conditions for a high volume fraction dyed PCCA of large particles (225 nm). Curves A and B were measured for the PCCA (sample B) with n_m adjusted to 1.3930 and 1.3803, respectively. The probe beam was delayed by 2.5 ns compared to the pump beam. The pump beam spot radius on the sample was ~50 μm.

focusing of the pump beam into the thin PCCA sample. The pump beam energy required to achieve T_g for sample B is more than two times lower than the corresponding energy for sample A (570 μJ). One reason is that the beam waist for sample B case (~50 μm) is smaller than sample A case (~100 μm). Another reason is that sample B has a larger absorption cross section (1.48×10^{-13} cm^2/particle) than sample A (2.98×10^{-14} cm^2/particle). Thus, the sample damage threshold for sample B (~600 μJ) is also lower than that of sample A (~1500 μJ). Curve A in Figure 9 shows that the R_{on}/R_{off} signal at T_g is ~1.7, which is very close to that predicted (1.8) by using eqs 10 and 11.

Thus, we have observed nanosecond optical switching for these mesoscopically periodic arrays. We expect that this switching phenomenon can be used for optical limiting if the dye absorption is coincident with the diffracted wavelength, or for optical switching where a pump beam would control the diffraction and transmission of one or more probe beams. In fact this device could be used for parallel optical switching since small areas of the PCCA could be individually addressed to

permit parallel processing. We expect that the pixel density could be quite high.

At present, however, the device switches only 2% of the probe beam, which is far below that theoretically expected. We calculated using Dynamical Diffraction Theory[9,15,18,19] that the diffraction efficiency for a perfect PCCA lattice should be 97% for the 600 μJ pump excitation that transiently heats the spheres to 60 °C. Since we independently verified[17] that our temperature and refractive index changes conform to our theoretical conditions, we ascribe the decreased Bragg diffraction efficiency to disorder in the PCCA lattice.

We are developing methods to prepare more perfect PCCA films. In addition, we recently discovered that we can increase the sphere scattering power by over 10-fold by using second-order diffraction.[19] Further optimization of these PCCA should lead to efficient optical switching devices and limiters. The unique potential efficiency of these devices results from the fact that this mesoscopically period array concentrates the scattering power of the particles into a narrow solid angle which fulfills the Bragg condition.

Conclusion

We prepared Bragg diffracting crystalline colloidal arrays of dyed poly(1H,1H-heptafluorobutyl methacrylate) spheres locked in polyacrylamide hydrogels. We refractive index matched the particles to the medium and measured the diffracted probe energy change as a function of pump beam heating of this PCCA. We demonstrated that this system will switch on diffraction in the nanosecond time regime. Theoretically, over 97% of the incident light should be diffracted. However, we observed a much smaller efficiency due to crystalline colloidal array disorder. We are now in the process of improving the array ordering.

Acknowledgment. We thank A. Tse for preparing the acylated Oil Blue N dye and providing the heat capacity data; P. Li, Z. Wu, J. Holtz, J. M. Weissman, and H. B. Sunkara for helpful discussions; and L. Liu for calculating the dynamical diffraction efficiencies. Supported by the Office of Naval Research through Grant No. N00014-94-0592 and by the National Science Foundation through Grant No. CHE 9633561.

Appendix

We here calculate the dependence of diffraction efficiency on the PCCA volume fraction. At the Bragg angle the ratio of the diffracted power (I_d) to the incident power (I_0) for a perfect crystal is[9]

$$I_D/I_0 = (\tanh A)^2 \tag{12}$$

where

$$A = \frac{2}{\pi 3^{3/2}} \frac{\kappa}{\lambda_0}\left(\frac{n}{n_0}\right)\left[\frac{3(m^2-1)}{m^2+2}\right](\sin u - u\cos u)\left(\frac{t_0}{\sin\theta_B}\right) \tag{13}$$

where κ is the polarization factor, n is the refractive index of the suspension, n_0 is the refractive index of air, t_0 is the single-crystal thickness, m is the refractive index ratio between the particle and the surrounding medium. u is the scattering size parameter:

$$u = \frac{2\pi n D_0 \sin\theta_B}{\lambda_0} \tag{14}$$

where D_0 is the particle diameter. From eqs 12 and 13, we can see that the diffraction intensity monotonically increases with A. Thus, to find maximum diffraction intensity we need to maximize A. We can set λ_0, m, t_0, and θ_B as constants and eq 13 becomes

$$A = K\mathrm{n}(\sin u - u\cos u) \tag{15}$$

where K is a constant, n is a linear function of the particle volume fraction as indicated in eq 3, which can be rearranged to

$$n = (n_p/m)[(m-1)\Phi_p + 1] \tag{16}$$

the size parameter u is also a function of the volume fraction. For FCC crystals, the relationship among the volume fraction, the nearest neighbor spacing (D), and the particle diameter (D_0) is[1]

$$\Phi_p\left(\frac{D}{D_0}\right)^3 = \frac{\pi}{3\times 2^{1/2}} = 74.05\% \tag{17}$$

The nearest neighbor interparticle spacing is given by

$$D = (3/2)^{1/2} d_{111} \tag{18}$$

Combining eqs 2, 14, 17, and 18, we have

$$\Phi_p = \frac{2}{(9\times 3^{1/2})\pi^2}\left(\frac{u}{M}\right)^3 = 0.013\,00(u/M)^3 \tag{19}$$

Since Φ_p is less than 74.06% (close-packed crystals), $u < 3.85$ for the first-order diffraction ($M = 1$). By combining eqs 15, 16, and 19, we have

$$A = K\,(n_p/m)[(m-1)k\,u^3 + 1]\,(\sin u - u\cos u) \tag{20}$$

where $k = 0.01300$. The volume fraction that maximizes A is determined by numerically solving the expression: $\mathrm{d}A/\mathrm{d}u = 0$. For the PFBMA particles ($m = 1.386/1.333$), $u = 3.157$, i.e., $\Phi_p = 40.9\%$. In contrast, for the high refractive index polystyrene colloidal particles ($m = 1.590/1.333$), $\Phi_p = 43.1\%$. Thus, the maximum diffraction condition is not highly sensitive to the particle refractive index mismatch from the medium. The maximum diffraction occurs under conditions where a maximum occurs in the modulation of the optical dielectric constants of the set of planes. We calculate that this diffraction maximum occurs below the close-packed limit volume fraction, where the sphere layers in the d_{111} planes are close to overlapping, but below the close-packed limit.

JA980481A

(19) Liu, L.; Li, P.; Asher, S. A. *J. Am. Chem. Soc*. **1997**, *119*, 2729−2732.